

Engineering Note

3-D Wheel: A Single Actuator Providing Three-Axis Control of Satellites

Jon Seddon* and Alexandre Pechev†
 University of Surrey, Guildford,
 England GU2 7XH, United Kingdom

DOI: 10.2514/1.A32039

I. Introduction

ACTIVE magnetic bearings (AMBs) offer many advantages for momentum wheels on small satellites compared with conventional bearings using ball or roller bearings. Conventional bearings require a form of lubricant, which evaporates in the vacuum of space unless sealed, or to be made from a dry lubricant. The bearings will wear with time and may eventually fail, limiting the lifetime of the satellite. To minimize the wear on its bearings, the wheel may be operated at a low spin rate, limiting the angular momentum of the wheel. Using AMBs means that there is no contact between moving parts, and so lubrication is not required and wear is not an issue [1]. As the resolution of the cameras in small satellites approaches 1 m ground resolution [2] microvibrations on the satellite increasingly affect the image quality. The bandwidth and precision of an AMB-based momentum wheel allow it to damp such microvibrations.

The number of degrees of freedom that are actively controlled can be chosen. The 3-D wheel presented here has 5 degrees of freedom actively controlled. Because the tilt angle of the wheel is actively controlled, it is possible to tilt the wheel, generating a gyroscopic output torque in a similar fashion to a control moment gyro (CMG). Unlike a CMG, the tilt axis of the 3-D wheel is not fixed, and the gyroscopic output torque can be steered to be anywhere in the plane normal to the spin axis of the wheel. A single wheel is therefore capable of generating an output torque about all three principle axes of the spacecraft. Because the wheel is tilted using electromagnets, it can be tilted at a high rate, generating a large output torque. The bandwidth of the gyroscopic torque is higher than a conventional momentum wheel's, making it ideal for the damping of microvibrations for highly sensitive payloads or for the rapid reorientation of spacecraft during maneuvers such as rendezvous and docking.

In this Note we present the design of the engineering model of the 3-D wheel that has been built: a tilting magnetically levitated momentum-wheel for small satellites. We discuss the design of the wheel and then present the results of testing this engineering model. The position of the wheel can be controlled to within $2.5 \mu\text{m}$ and the tilt angle can be controlled with an accuracy of 0.1 mrad. The bandwidth of the wheel and controller is 120 rad/s. The wheel can be tilted at a maximum rate of 0.56 rad/s, which when the wheel is spinning at 5000 rpm generates a gyroscopic output torque of $0.68 \text{ N} \cdot \text{m}$. The design is scalable; the diameter of the rotor can be increased for a larger moment of inertia and a greater torque generation capability.

Received 31 January 2011; accepted for publication 26 November 2011. Copyright © 2012 by Jon Seddon. Published by the American Institute of Aeronautics and Astronautics, Inc., with permission. Copies of this paper may be made for personal or internal use, on condition that the copier pay the \$10.00 per-copy fee to the Copyright Clearance Center, Inc., 222 Rosewood Drive, Danvers, MA 01923; include the code 0022-4650/12 and \$10.00 in correspondence with the CCC.

*Ph.D. Student, Surrey Space Centre; j.seddon@surrey.ac.uk.

†Lecturer, Surrey Space Centre; a.pechev@surrey.ac.uk.

II. Wheel Design

The approach taken by the authors uses the electromagnetic principle for the active magnetic bearing, which has the benefit of being able to generate larger forces providing an increased stiffness [3]. Previous wheels have used the electrodynamic principle [4–7], which has the benefit of a linear relationship between force and current [8,9]; modern control techniques are able to overcome this nonlinearity [10–13].

Figure 1 shows the arrangement of the electromagnets around the rotor in the 3-D wheel. The geometry of the rotor and electromagnets was optimized using an analytical model of the wheel and three-dimensional magnetostatic finite element simulations as shown in Fig. 2. The range of angles that the wheel can tilt through is controlled by the width of the air gap between the electromagnets and the rotor. The attractive reluctance force generated by an electromagnet on a steel rotor is given by [14,15]

$$F_{\text{rel}} = -\frac{\mu_0 N^2 \epsilon l i^2}{4\gamma^2} \quad (1)$$

where μ_0 is the permeability of free space, N is the number of turns in the electromagnet's coil, ϵl is the cross-sectional area of the electromagnet's pole face, i is the current flowing through the coils, and γ is the width of the air gap between the electromagnet's pole face and the rotor's pole face.

Using small angle approximations, the air gap width γ in meters is $\gamma = \theta r_h / 2$ where θ is the maximum angle to be tilted through in radian and r_h is the height of the rotor in meters. For a wheel 56 mm high, a tilt range of ± 3 deg requires an air gap width of 1.5 mm, and a tilt range of ± 5 deg requires an air gap width of 2.6 mm. Because the force generated by the electromagnets and hence the stiffness of the bearing is proportional to $1/\gamma^2$ the maximum tilt range of the wheel is limited. The engineering model was built with an air gap width of 1.4 mm giving a tilt range of ± 2.7 deg. The limited tilt range means that the gyroscopic output torque can only be sustained for a short period of time, but because it is generated by the electromagnets it has a high bandwidth.

For the engineering model shown in Fig. 1, the electromagnets were placed around the outside of the wheel to allow the coils to be wound easily. A more compact flight model would have the electromagnets in the center of the wheel. Finite element simulations show that this would not change the performance of the wheel. The steel stator pieces are made from laminated steel to minimize eddy current losses; the rotor is solid steel.

The wheel's translational and rotational positions are measured by five Sensonics PRS04 contactless eddy current sensors with a resolution of $2.0 \mu\text{m}$. The controller is implemented on a real-time control system. The current amplifiers were designed by Delft Technical University, Netherlands, using class A amplifiers. For the engineering model they allowed a low-noise current amplifier to be quickly built, but have a poor power efficiency and would not be used on a flight model of the wheel. The spin rate of the wheel is measured using a Hall effect sensor.

The initial controller used assumes that the rotational and translational motion along and about each axis is decoupled from all other motion. To make this assumption valid the gyroscopic coupling between rotational axes is assumed to be a disturbance. The linearized attractive reluctance force generated by a single electromagnet is

$$\begin{aligned} F_{\text{rel}} &= \frac{\mu_0 N^2 \epsilon l i_0^2}{4\gamma_0^2} + \frac{\mu_0 N^2 \epsilon l i_0}{2\gamma_0^2} \Delta i - \frac{\mu_0 N^2 \epsilon l i_0^2}{2\gamma_0^3} \Delta \gamma \\ &= f_0 + K_i \Delta i - K_\gamma \Delta \gamma \end{aligned} \quad (2)$$

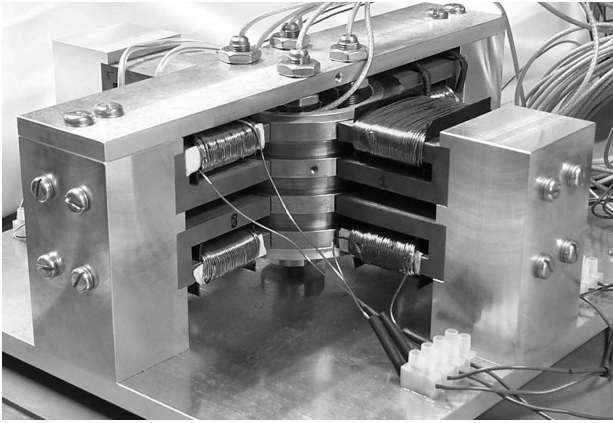


Fig. 1 The engineering model of the wheel.

Then, the translational force on the rotor along the x axis produced by four electromagnets is

$$F_x = f_1 + f_2 - f_5 - f_6 = 4K_i \Delta i_x + 4K_y \Delta x \quad (3)$$

Using Newton's second law and applying the Laplace transform, we have the following transfer function:

$$G_x(s) = \frac{X(s)}{i_x(s)} = \frac{4K_i/M}{s^2 - 4K_y/M} \quad (4)$$

Similarly, for a rotation about the y axis by an angle α_y ,

$$T_y = r_z(f_1 + f_6 - f_2 - f_5) = 4r_z K_i \Delta i_{\alpha_y} + 4r_z^2 K_y \Delta \alpha_y \quad (5)$$

assuming the rotor's inertia matrix is diagonal,

$$G_{\alpha_y}(s) = \frac{A_y(s)}{i_{\alpha_y}(s)} = \frac{4r_z K_i / I_{yy}}{s^2 - 4r_z^2 K_y / I_{yy}} \quad (6)$$

The transfer functions for rotation and translation are both double integrators in the range of frequencies of interest with a constant phase angle of -180 deg. Compensators were generated to stabilize the translational motion and the rotational motion. The error between the desired and measured translation or rotation is fed to the input of the compensator and the output is the Δi for motion along or about that axis. The current to electromagnet 1 is $i_1 = i_0 + i_x + i_{\alpha_y}$ and the currents for the other electromagnets can be derived similarly.

Initially lead-lag compensators were used. The experimental responses around the operating point were measured using frequency domain analysis with hardware in the loop testing. Additional unmodeled dynamics of the system were identified. The phase margin achievable with the first-order lead-lag compensator was not high enough to guarantee stability. Therefore a similar decoupled controller was generated using H_∞ sensitivity minimization using the analytical model derived with the additional dynamics from the frequency domain analysis included. This controller gave 39 deg of phase margin at the crossover frequency of 114 rad/s for rotational motion. The transfer function of the synthesized rotational controller before discretization is

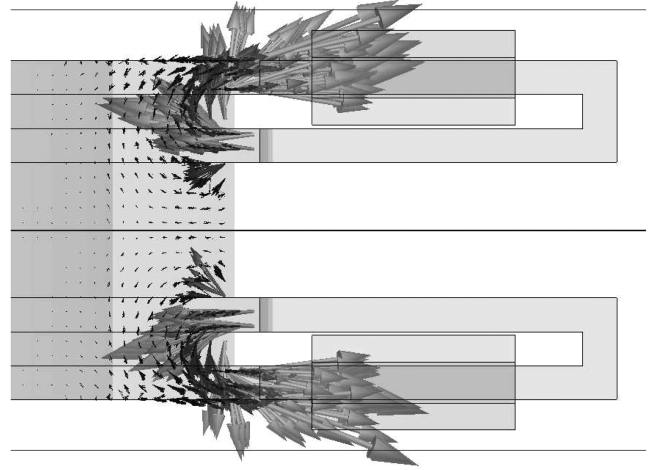


Fig. 2 A three-dimensional finite element simulation of two electromagnets and part of the rotor. The direction of the arrows indicates the direction of flux and the size of the arrows the magnitude of the flux density.

III. Results

Figure 3 shows the wheel being translated by a step demand of $2.5 \mu\text{m}$ along the x axis at time 15.0 s and separately being rotated about the y axis by a demand of 0.1 mrad at time 20.0 s. The analogue input card has a resolution of 12-bit, with one bit corresponding to $2.4 \mu\text{m}$. The quantization of the position is visible, showing that the system is low-noise and can be controlled with a high precision. The precision of this engineering model is limited by the resolution of the data acquisition card. Figure 4 shows the distribution of the wheel position during 14 s of levitation. The desired position is maintained to one sigma of the desired position within 3.9 microns and to within three sigma by 11.6 microns.

Figure 5 shows the tilt angle of the wheel as it is tilted through 0.03 rad (1.7 deg) at time 70.0 s while spinning at 496 rpm. It tilts through 0.0301 rad in 0.054 s at a rate of 0.558 rad/s. This generates a peak torque of $0.067 \text{ N} \cdot \text{m}$ at 496 rpm, or would generate a torque of $0.680 \text{ N} \cdot \text{m}$ if this tilt rate is sustained while the wheel is rotating at 5000 rpm. The frequency of the periodic disturbance in the tilt angles about both axes is the same as the rotor's angular velocity. This disturbance is due to the component of the spinning rotor's angular velocity about the x axis, which is gyroscopically coupled to the y axis. Additional feedback terms will be added to the controller to reduce this disturbance.

To demonstrate its conventional torque capability the rotor was accelerated from 0 to 80 rad/s (760 rpm), which took 10 s. This acceleration generates a torque of at least $0.02 \text{ N} \cdot \text{m}$ for the duration of the acceleration with a peak torque of $0.037 \text{ N} \cdot \text{m}$. The brushless dc motor fitted to the engineering model of the wheel is designed for another application and is not optimized for this wheel. With an optimized motor this torque can either be increased, or maintained with a lower power consumption. This torque is comparable to existing similar sized conventional momentum wheels for small satellites. The wheel was not spun faster than 80 rad/s because it had not been balanced and the disturbance forces due to its static and couple mass imbalance prevented it from spinning faster than this.

Figure 6 shows the frequency response of the wheel hardware measured experimentally. The crossover frequency of the response was 114 rad/s. The bandwidth of this wheel is two orders of magnitude greater than could be achieved using a conventional wheel accelerating the rotor around mechanical bearings [16].

$$K_\alpha(s) = \frac{2245995927(s + 3030)(s + 454.5)(s + 58.2)(s + 16.5)(s^2 + 5760s + 1.296 \times 10^7)}{s(s + 4.11 \times 10^4)(s + 4733)(s^2 + 1530s + 8.079 \times 10^6)(s^2 + 6977s + 2.031 \times 10^7)} \quad (7)$$

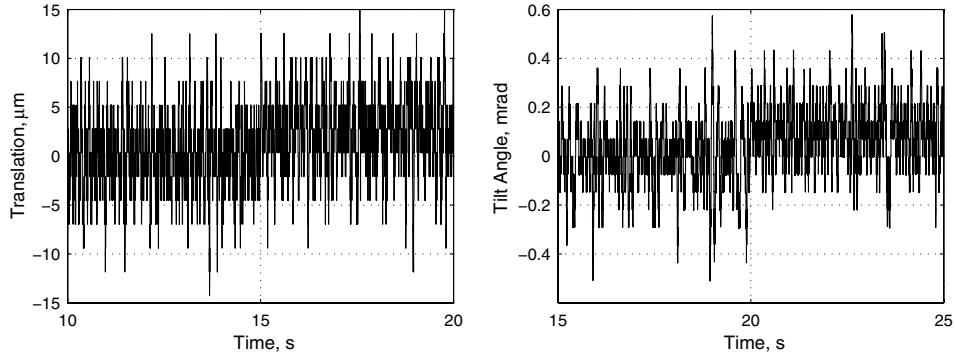


Fig. 3 A 2.5 μm translation demanded along the x-axis at 15.0 s and a separate 0.1 mrad rotation demanded about the y-axis at 20.0 s.

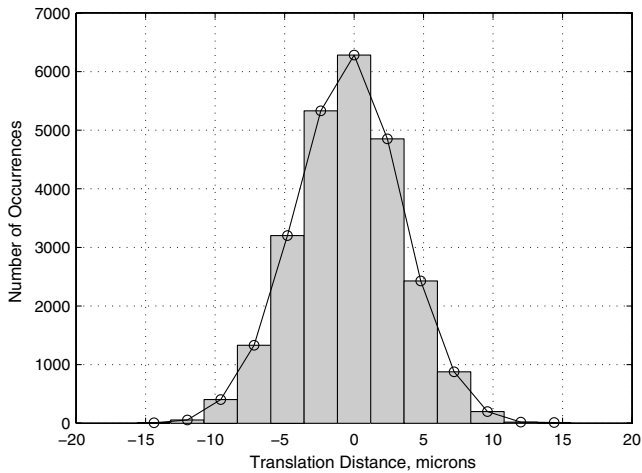


Fig. 4 The distribution of the wheel positions from the central position during levitation.

IV. Conclusions

An engineering model of a tilting magnetically levitated momentum-wheel that is capable of generating an output torque about all three principle axes of a spacecraft using a single wheel has been built and demonstrated. The wheel uses the electromagnetic principle providing additional flexibility compared with previous designs. The bandwidth of the output torque is two orders of magnitude greater than is available from a conventional momentum wheel. This makes it ideal for damping microvibrations in high-resolution imaging satellites, such as those approaching 1 m ground

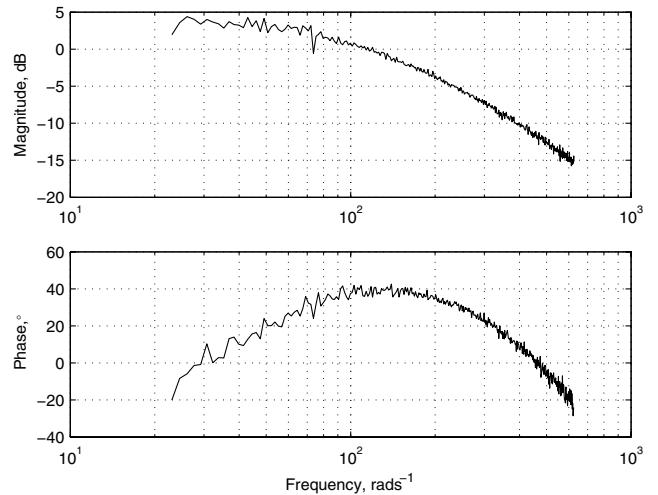


Fig. 6 The measured frequency response for rotations about the x-axis.

resolution, where the increasing resolution requires a lower noise level platform to obtain the desired image quality. Existing actuators cannot damp the high-frequency vibrations that this wheel can. The ability to generate an output torque about all three axes can improve the redundancy, or provide mass and power savings. All magnetically levitated momentum-wheels have the benefits, when compared with conventional wheels, of not requiring lubrication and having no moving parts in contact, providing a longer lifetime. Further work will add additional terms to the controller to improve its performance; a balanced rotor will be used to demonstrate levitation at all angular velocities.

References

- [1] Henrikson, C. H., Lyman, J., and Studer, P. A., "Magnetically Suspended Momentum Wheels for Spacecraft Stabilization," *12th AIAA Aerospace Sciences Meeting*, AIAA, Washington, D. C., 1974, pp. 1–8.
- [2] Cutter, M., Davies, P., Baker, A., and Sweeting, M., "A High Performance EO Small Satellite Platform and Optical Sensor Suite," *IEEE Geoscience and Remote Sensing Symposium*, IEEE Publications, Piscataway, NJ, , 2007, pp. 3851–3854.
- [3] Sindlinger, R., "Magnetic Bearing Momentum Wheels with Magnetic Gimbaling Capability for 3-Axis Active Attitude Control and Energy Storage," *Attitude and Orbit Control Systems Conference*, ESA Rept. No. SP-128, Noordwijk, The Netherlands, 1977, pp. 395–401.
- [4] Studer, P., "A Practical Magnetic Bearing," *IEEE Transactions on Magnetics*, Vol. 13, No. 5, 1977, pp. 1155–1157. doi:10.1109/TMAG.1977.1059690
- [5] Murakami, C., Ohkami, Y., Okamoto, O., Nakajima, A., Inoue, M., Tsuchiya, J., Yabu-Uchi, K., Akishita, S., and Kida, T., "A New Type of Magnetic Gimballed Momentum Wheel and its Application to Attitude Control in Space," *Acta Astronautica*, Vol. 11, No. 9, 1984, pp. 613–619. doi:10.1016/0094-5765(84)90036-5

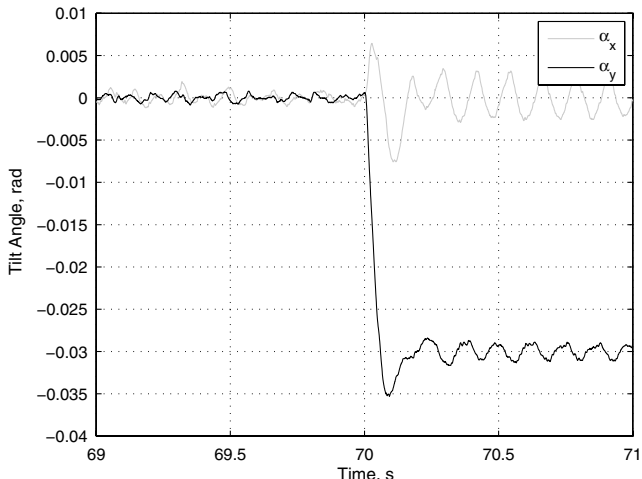


Fig. 5 The wheel's tilt angle, while tilting the wheel through 0.03 rad and spinning at 496 rpm.

- [6] Scharfe, M., Meinzer, K., and Zimmermann, R., "Development of a Magnetic-Bearing Momentum Wheel for the AMSAT Phase 3-D Small Satellite," *International Symposium on Small Satellites*, CNES, Paris, 1996.
- [7] Scharfe, M., Roschke, T., Bindl, E., Blonski, D., and Seiler, R., "The Challenges of Miniaturisation for a Magnetic Bearing Wheel," *Proceedings of the 9th European Space Mechanisms and Tribology Symposium*, ESA, Noordwijk, The Netherlands, 2001, pp. 17–24.
- [8] Gerlach, B., Ehinger, M., Raue, H. K., and Seiler, R., "Gimballing Magnetic Bearing Reaction Wheel with Digital Controller," *11th European Space Mechanisms and Tribology Symposium, ESMATS 2005*, ESA, Noordwijk, The Netherlands, 2005, pp. 35–40.
- [9] Allaire, P. E., Maslen, E. H., Humphris, R. R., Sortore, C. K., and Studer, P. A., "Low Power Magnetic Bearing Design For High Speed Rotating Machinery," *International Symposium on Magnetic Suspension Technology*, NASA N92-27721 18–18, 1991.
- [10] Shafai, B., Beale, S., Larocca, P., and Cusson, E., "Magnetic Bearing Control Systems and Adaptive Forced Balancing," *IEEE Control Systems Magazine*, Vol. 14, No. 2, 1994, pp. 4–13. doi:10.1109/37.272775
- [11] Tsiotras, P., and Wilson, B. C., "Zero and Low-Bias Control Designs for Active Magnetic Bearings," *IEEE Transactions on Control Systems Technology*, Vol. 11, No. 6, 2003, pp. 889–904. doi:10.1109/TCST.2003.819593
- [12] Lindlau, J. D., and Knospe, C. R., "Feedback Linearization of an Active Magnetic Bearing with Voltage Control," *IEEE Transactions on Control Systems Technology*, Vol. 10, No. 1, 2002, pp. 21–31. doi:10.1109/87.974335
- [13] Lanzon, A., and Tsiotras, P., "A Combined Application of H-infinity Loop Shaping and mu-Synthesis to Control High-Speed Flywheels," *IEEE Transactions on Control Systems Technology*, Vol. 13, No. 5, 2005, pp. 766–77. doi:10.1109/TCST.2005.847344
- [14] Molenaar, L., "A Novel Planar Magnetic Bearing and Motor Configuration Applied in a Positioning Stage," Ph.D. Thesis, Technische Universiteit Delft, 2000.
- [15] Demarest, K. R., *Engineering Electromagnetics*, Prentice-Hall, Upper Saddle River, NJ, 1998.
- [16] Seddon, J., and Pechev, A., "A Low-Noise, High-Bandwidth Magnetically-Levitated Momentum-Wheel for 3-Axis Attitude Control from a Single Wheel," *13th European Space Mechanisms and Tribology Symposium 2009*, Vol. SP670, ESA, Noordwijk, The Netherlands, 2009.

G. Agnes
Associate Editor